

such as σ_{C-X}^* and σ_{XH}^* . Since these empty orbitals are at lower energy when X = S, this effect favors the second-row substituent, as observed above.

4. Conclusion

In this paper we have attempted to rationalize the trends of the stabilization energies of the α -substituted oxy- and thio-carbanions $H_2\bar{C}-OH$ and $H_2\bar{C}-SH$. To this purpose we have decomposed the stabilization energies into the component terms associated with the σ -effects, the nonbonded interaction effects, the 3d-orbitals effects, and the correlation energy effects.

The analysis has shown that at all levels of computations investigated the SH group stabilizes the anionic center more than the OH group and that this trend is determined by the σ effects.

An OEMO rationalization of this effect has shown that the stabilization energy of the SH group is larger because the bond weakening associated with the removal of a proton in the H_3C- fragment is more significant for X = OH than for X = SH. In turn, this trend is determined by the matrix element, which, in going from the monosubstituted methane to the related anion, is reduced more in the oxy than in the thio derivatives.

The analysis has shown also that the effect of the nonbonded interactions favors OH vs. SH and that the contribution of the sulfur 3d orbitals is very small. More significant appears to be the contribution associated with the correlation energy effects, which favors SH over OH.

Registry No. $^-CH_2OH$, 55830-71-2; $^-CH_2SH$, 51422-57-2.

Catalysis of Electrochemical Reactions at Redox Polymer Coated Electrodes. Mediation of the Fe(III)/Fe(II) Oxido-Reduction by a Polyvinylpyridine Polymer Containing Coordinatively Attached Bisbipyridine Chlororuthenium Redox Centers

Claude P. Andrieux, Otto Haas,¹ and Jean-Michel Savéant*

Contribution from the Laboratoire d'Electrochimie Moléculaire de l'Université de Paris 7, Unité Associée au CNRS No. 438, 75251 Paris, Cedex 05, France. Received May 19, 1986

Abstract: The $[Ru(bpy)_2Cl-poly(4-vinylpyridine)]$ redox polymer catalyzes the oxidation of Fe(II) into Fe(III) in 1 M HCl in a quite efficient manner both in terms of current and potential. Quite substantial portions of the film thickness are active in the catalytic system, providing a good example of the interest of redox polymer coatings in the catalysis of electrochemical reactions as a result of the three-dimensional dispersion of the reacting centers. The polymer is also able to catalyze, although to a lesser extent, the reduction of Fe(III) to Fe(II) in the same medium in spite of the fact that the standard potential of the Ru(III)/Ru(II) couple is positive to that of the Fe(III)/Fe(II) couple. Analysis of the experimental data and the optimization of the catalytic efficiency by means of previously developed kinetic models demonstrate the validity of these models both in terms of the limiting currents and half-wave potentials featuring the catalytic process.

Redox polymer coated electrodes have been the object of active investigation during the past 10 years, motivated mainly by their applications to the catalysis of electrochemical reactions (for recent reviews see ref 2). The main reason for the interest they aroused in this respect is the expectation that they may combine the advantages of monolayer derivatized electrodes with those of homogeneous catalytic systems. With redox polymer coatings as with monolayer derivatized surfaces, high local concentrations of catalytic sites can be achieved even though the total amount of catalyst remains small. The two systems also share the advantage of an easy separability of the reaction products from the catalyst. On the other hand, redox polymer coatings, as homogeneous catalytic systems, offer a three-dimensional dispersion of the reacting centers as opposed to the two-dimensional arrangement prevailing at bare electrodes and at monolayer derivatized surfaces.³ It follows that catalytic efficiencies of redox

polymer coatings are expected to increase with the amount of redox polymer deposited on the electrode surface.³ However, this potentiality may be counteracted by limitations imposed by the rates of substrate diffusion and charge propagation across the coatings. These may indeed be so severe that the catalytic reaction becomes a surface process occurring at either the coating-solution or the electrode-coating interfaces. Under such circumstances, monolayer derivatized surfaces may prove more efficient than redox

(3) (a) This is the reason why catalysis can be obtained with redox polymer coatings and homogeneous systems, but not with monolayer derivatized surfaces, even in the cases where the catalyst simply exchanges electrons in an outer-sphere manner with the substrate.^{3b,c} This "redox catalysis"^{3d} thus results from physical rather than chemical reasons. In the case of "chemical catalysis",^{3d-e} where an essential step is the transient formation of an adduct between the catalyst and the substrate, catalysis occurs at monolayer derivatized surfaces as a consequence of their particular chemical properties. The potential advantage of redox polymer coatings is then the possible multiplication of the effect as the number of equivalent monolayers of catalyst increases.^{3b} (b) Andrieux, C. P.; Savéant, J. M. *J. Electroanal. Chem.* **1978**, *93*, 163. (c) Andrieux, C. P.; Dumas-Bouchiat, J. M.; Savéant, J. M. *Ibid.* **1981**, *123*, 171. (d) Andrieux, C. P.; Dumas-Bouchiat, J. M.; Savéant, J. M. *Ibid.* **1978**, *87*, 39. (e) Lexa, D.; Savéant, J. M.; Soufflet, J. P. *Ibid.* **1979**, *100*, 159. (f) Anson, F. C.; Ni, C. L.; Savéant, J. M. *J. Am. Chem. Soc.* **1985**, *107*, 3442. (g) Lexa, D.; Savéant, J. M.; Wang, D. L. *Organometallics* **1986**, *5*, 7428.

(1) Present address: Swiss Federal Institute for Reactor Research, CH-5303 Wuerenlingen, Switzerland.

(2) (a) Albery, W. J.; Hillman, A. R. *Annual Reports C.* (1981); The Royal Society: London, 1983, pp 317-437. (b) Murray, R. W. *Electroanalytical Chemistry*; Bard, A. J., Ed.; Marcel Dekker, New York, 1984; Vol. 13, pp 191-368.

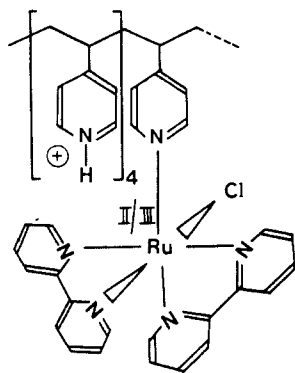


Figure 1. Chemical structure of the ruthenium polymer.

polymer coatings owing to limitation of the current by charge propagation in the first case and substrate diffusion in the second.

Kinetic models have been developed for steady-state regimes that allow one to identify the rate-controlling factors, to describe their interplay, to extract the pertinent kinetic constants from the experimental data, and to optimize the catalytic efficiency of the polymer coating. Rigorous treatments have been given for the case of simple catalytic schemes involving a single irreversible⁴ or reversible rate-determining step in the catalytic process.⁵ More complicated schemes, as frequently encountered in chemical catalysis, have also been analyzed.⁶ These models are based on the fact that, besides the transport of the substrate from the bulk of the solution to the solution-coating interface, the current is governed by three rate-limiting phenomena in the polymer film: the catalytic reaction itself (R), the diffusion-like charge propagation (E), and the substrate diffusion⁷ (S) across the coating.⁸

The validity of these models has been tested in several experimental examples both in the case where the catalytic reaction takes place within the outermost monolayers of the coating⁹ and, more interestingly, in that where a macroscopic portion of the coating is catalytically active.¹⁰ The investigations carried out

with the latter systems have exclusively concerned the catalytic plateau currents and not the potential location of the waves in spite of theoretical indications allowing the treatment of this aspect of the problem.^{5a} The question of the potential location of the catalytic wave is actually an important element in the evaluation of the catalytic efficiency to be combined with the data regarding the magnitude of the catalytic current. For these reasons and also because only a small number of experimental systems have been tested so far, the investigation of novel experimental examples appears desirable.

Among redox polymer coatings on electrodes, those containing ruthenium complexes as electroactive centers have received particular intense attention, presumably because of their photoelectrochemical potentialities. Two modes of attachment of the ruthenium complexes to the polymer were used: coordinative attachment to a ligand (often a pyridine) pendent from the polymer backbone;¹¹ electrostatic attachment of a positive ruthenium complex to a negatively charged polyelectrolyte (Nafion,^{3f,9f,12,13} poly(vinyl sulfonate),¹⁴ clays¹⁵). The catalytic properties of several of these ruthenium-containing polymer coatings have been analyzed using the above-mentioned kinetic models. However, with the exception of one particular case,¹⁶ the catalytic reaction has been shown to occur at the coating/solution boundary because of insufficient penetration of the substrate into the polymer film.⁹

We report hereafter a quantitative analysis of the catalytic properties of the ruthenium containing polymer depicted in Figure 1. Its preparation and a qualitative description of several of its electrochemical and photochemical characteristics have been already given.¹⁷ The reaction we investigated as an example is the oxidation of iron(II) to iron(III) in concentrated hydrochloric acid solutions (1 M). Quite large catalytic effects involving a substantial portion of the coating were obtained. The variations of the plateau current as well as of the potential location of the wave will be analyzed. It is interesting to note that the reverse reaction, i.e., the reduction of iron(III) to iron(II), can also be mediated by the same polymeric coating, although to a much lesser extent in spite of the fact that the Ru(III)/Ru(II) standard potential is positive to that of the Fe(III)/Fe(II) couple. The variations of both the plateau current and of the half-wave potential will also be analyzed in this case.

(4) (a) Andrieux, C. P.; Savéant, J. M. *J. Electroanal. Chem.* **1978**, *93*, 163. (b) Andrieux, C. P.; Dumas-Bouchiat, J. M.; Savéant, J. M. *Ibid.* **1980**, *114*, 159. (c) Andrieux, C. P.; Dumas-Bouchiat, J. M.; Savéant, J. M. *Ibid.* **1981**, *123*, 343. (d) Andrieux, C. P.; Dumas-Bouchiat, J. M.; Savéant, J. M. *Ibid.* **1982**, *131*, 1. (e) Andrieux, C. P.; Savéant, J. M. *Ibid.* **1982**, *134*, 163. (f) Andrieux, C. P.; Savéant, J. M. *Ibid.* **1984**, *169*, 9. (g) Albery, W. J.; Hillman, R. A. *Ibid.* **1984**, *170*, 27. (h) Leddy, J.; Bard, A. J.; Maloy, J. T.; Savéant, J. M. *Ibid.* **1985**, *187*, 205.

(5) (a) Andrieux, C. P.; Savéant, J. M. *J. Electroanal. Chem.* **1982**, *142*, 1. (b) Anson, F. C.; Savéant, J. M.; Shigehara, K. *J. Phys. Chem.* **1983**, *87*, 214.

(6) Andrieux, C. P.; Savéant, J. M. *J. Electroanal. Chem.* **1984**, *171*, 65.

(7) In most cases the partition of the substrate between the solution and the coating has been assumed to be fast enough for equilibrium to be achieved. Slow crossing of the solution-coating boundary can, however, be introduced as an additional rate-limiting factor in the treatment.^{4h}

(8) (a) It is convenient to represent each rate-limiting factor by a characteristic current density:^{4e,f,h,5a} diffusion of the substrate in the solution, $i_A = FDC_A^0/\delta$; diffusion of the substrate across the coating, $i_S = FD_S C_A^0/\phi$; diffusion-like charge propagation across the coating, $i_E = FD_E C_P^0/\phi$; catalytic reaction, $i_k = FkC_A^0 C_P^0 \phi = kC_A^0 \Gamma_P^0$, where D , D_S , D_E stand for the corresponding diffusion coefficients; C_A^0 is the bulk concentration of the substrate (A), C_P^0 the concentration of the catalyst in the film, Γ_P^0 the amount of catalyst deposited on the electrode per unit surface area, κ the partition coefficient of the substrate between the solution and the coating;⁷ k the rate constant of the rate-determining step of the catalytic process,^{8b} ϕ the film thickness, and δ the solution diffusion layer thickness. (b) For a single irreversible catalytic step, a single parameter, i_k , is sufficient for representing the reaction. For a single reversible step a second parameter, e.g., the equilibrium constant, is required.^{5a} Likewise for a two-step catalytic process, a second parameter representing the competition between the two steps is necessary.⁶

(9) (a) Ikeda, T.; Leidner, C. R.; Murray, R. W. *J. Am. Chem. Soc.* **1981**, *103*, 7422. (b) Ikeda, T.; Leidner, C. R.; Murray, R. W. *J. Electroanal. Chem.* **1982**, *138*, 343. (c) Schmehl, R. H.; Murray, R. W. *Ibid.* **1983**, *152*, 97. (d) Leidner, C. R.; Murray, R. W. *J. Am. Chem. Soc.* **1984**, *106*, 1606. (e) Ewing, A. G.; Feldman, B. J.; Murray, R. W. *J. Electroanal. Chem.* **1984**, *172*, 145. (f) Krishnan, M.; Zhang, X.; Bard, A. J. *J. Am. Chem. Soc.* **1984**, *106*, 7371, 8329. (g) Anson, F. C.; Tsou, Y. M.; Savéant, J. M. *J. Electroanal. Chem.* **1984**, *178*, 113.

(10) (a) Both for redox^{3d,10b-f} and chemical catalysis processes.^{3f} (b) Oyama, N.; Anson, F. C. *Anal. Chem.* **1980**, *52*, 1192. (c) Kuo, K. N.; Murray, R. W. *J. Electroanal. Chem.* **1982**, *131*, 37. (d) Anson, F. C.; Savéant, J. M.; Shigehara, K. *J. Am. Chem. Soc.* **1983**, *105*, 1096. (e) Anson, F. C.; Savéant, J. M.; Shigehara, K. *J. Electroanal. Chem.* **1983**, *145*, 423. (f) Anson, F. C.; Oshaka, T.; Savéant, J. M. *J. Am. Chem. Soc.* **1983**, *105*, 4883.

(11) A detailed review of the preparation and properties of these polymers can be found in ref 2b, pp 305-314.

(12) (a) Buttry, D. A.; Anson, F. C. *J. Electroanal. Chem.* **1981**, *130*, 333. (b) Buttry, D. A.; Anson, F. C. *J. Am. Chem. Soc.* **1983**, *105*, 685. (c) Buttry, D. A.; Anson, F. C. *Ibid.* **1984**, *106*, 59. (d) McHatton, R. C.; Anson, F. C. *Inorg. Chem.* **1984**, *23*, 3925.

(13) (a) Rubinstein, I.; Bard, A. J. *J. Am. Chem. Soc.* **1980**, *102*, 6641. (b) Rubinstein, I.; Bard, A. J. *Ibid.* **1981**, *103*, 5007. (c) White, H. S.; Leddy, J.; Bard, A. J. *Ibid.* **1982**, *104*, 4811. (d) Martin, C. R.; Rubinstein, I.; Bard, A. J. *Ibid.* **1982**, *104*, 4817. (e) Leddy, J.; Bard, A. J. *J. Electroanal. Chem.* **1985**, *189*, 203.

(14) (a) Shaw, B. R.; Haight, G. P.; Faulkner, L. R. *J. Electroanal. Chem.* **1982**, *140*, 147. (b) Majda, M.; Faulkner, L. R. *Ibid.* **1982**, *137*, 149. (c) Majda, M.; Faulkner, L. R. *Ibid.* **1984**, *169*, 77. (d) Majda, M.; Faulkner, L. R. *Ibid.* **1984**, *169*, 97.

(15) (a) Gosh, P. K.; Mau, A. W. H.; Bard, A. J. *J. Electroanal. Chem.* **1984**, *169*, 315. (b) Ege, D.; Gosh, P. K.; White, J. P.; Equey, J. F.; Bard, A. J. *J. Am. Chem. Soc.* **1985**, *107*, 5644. (c) Rudzinski, W. E.; Bard, A. J. *J. Electroanal. Chem.* **1986**, *199*, 323.

(16) Dioxigen, as catalytically reduced by a cobalt porphyrin incorporated in a Nafion coating, electrons being shuttled from the electrode to the catalytic centers by a ruthenium hexaammine redox couple electrostatically bound to the polymer.^{3f}

(17) (a) Haas, O.; Vos, J. G. *J. Electroanal. Chem.* **1980**, *113*, 139. (b) Haas, O.; Kriens, M.; Vos, J. G. *J. Am. Chem. Soc.* **1981**, *103*, 1313. (c) Haas, O.; Muller, N.; Gerischer, H. *Electrochim. Acta* **1982**, *27*, 991. (d) Haas, O.; Zumbrennen, H. R.; Vos, J. G. *Ibid.* **1985**, *30*, 1551.

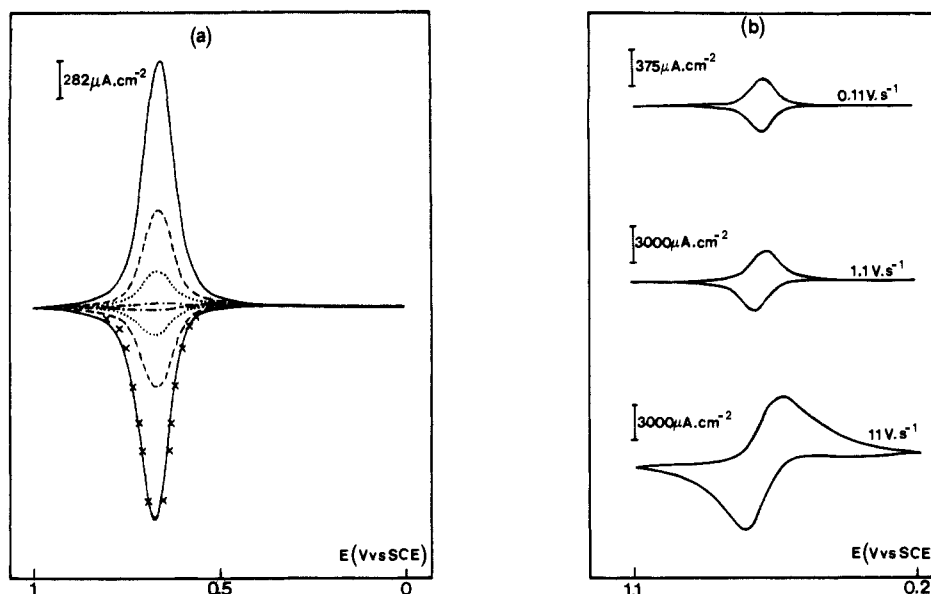


Figure 2. Cyclic voltammetry of the ruthenium polymer coating as a function of the surface concentration of ruthenium (Γ_p°) and the sweep rate: (a) sweep rate (0.1 V s^{-1}) from top to bottom, Γ_p° (M cm^{-2}) 2.4×10^{-8} , 8.6×10^{-9} , 3.2×10^{-9} , 3.1×10^{-10} ; points, theoretical curve (see text). (b) $\Gamma_p^\circ = 3.2 \times 10^{-9} \text{ M cm}^{-2}$; supporting electrolyte HCl 1 M in water.

Results and Discussion

Electrochemistry of the Attached Ru(III)/Ru(II) Couple. Redox Charge Transport in the Polymer Coating. Figure 2 shows the cyclic voltammetric behavior of the polymer in 1 M HCl as a function of the amount of polymer deposited on the electrode, Γ_p° , and of the sweep rate, v . At low sweep rate, the voltammograms exhibit the classical symmetric shape featuring the reversible reduction and oxidation of surface-confined reactants¹⁸ with an apparent standard potential equal to 0.685 V vs. SCE. Upon raising the sweep rate, a tailing of the wave occurs, characteristic of the appearance of the diffusion-like propagation of the charge across the coating.¹⁹

Closer inspection of the cyclic voltammograms obtained at low sweep rate (Figure 2a) reveals that, although the wave is symmetrical and reversible and has a height proportional to Γ_p° , the peak current and the wave width do not match exactly the theoretical equation:¹⁸

$$i = \frac{F^2}{RT} \Gamma_p^\circ v \frac{\exp[(F/RT)(E - E_{PQ}^\circ)]}{\{1 + \exp[(F/RT)(E - E_{PQ}^\circ)]\}^2} \quad (1)$$

(i = current density, E = electrode potential, E_{PQ}° = standard potential of the Ru(III)/Ru(II) couple). As discussed in detail in the case of another coordinatively attached ruthenium polymer,^{9b} this discrepancy can be assigned to activity effects involving electrostatic self- and cross-interactions between the Ru(III)²⁺ and Ru(II)⁺ ions. A satisfactory fitting of the experimental data with the corresponding equation

$$i = \frac{F^2}{RT} \Gamma_p^\circ v \frac{\left(1 - \frac{C_p}{C_p^\circ}\right) \frac{C_p}{C_p^\circ}}{1 - G \left(1 - \frac{C_p}{C_p^\circ}\right) \frac{C_p}{C_p^\circ}}$$

$$E = E^* + \frac{RT}{2F} \left(1 - \frac{2C_p}{C_p^\circ}\right) G + \frac{RT}{F} \ln \frac{C_p}{C_p^\circ - C_p}$$

with

$$E^* = E_{PQ}^\circ + \frac{RT}{2F} [(a_{QQ} + a_{QP}) - (a_{PP} + a_{PQ})]$$

$$G = [(a_{PP} + a_{QQ}) - (a_{PQ} + a_{QP})] C_p^\circ$$

(C_p° is the total concentration, C_p is the concentration of the oxidized form of the redox couple, and the a 's are the parameters describing the interactions between the various ions²⁰) is obtained as shown in Figure 2a. The value of the interaction parameter, $G = -0.62$, used for obtaining the fitting is small, much smaller than in the case of the other polyvinylpyridine polymer^{9b} mentioned above. This can be explained by the fact that the present polymer contains electroinactive ions (protonated pyridine) attached to the polymer backbone besides the ruthenium ions (Figure 1) which was not the case with the other ruthenium polymer. These attached electroinactive ions play the role of a supporting electrolyte which tends to minimize the variations of the electroactive ions activity coefficients as the redox composition of the film is changed. As seen in the next sections, the variations of the activity coefficients have a negligible influence on the potential location of the catalytic waves obtained with the Fe(III)/Fe(II) couple is rotating disk electrode voltammetry (RDEV).

An estimate of the rate of charge propagation can be derived from the diffusion character taken by the cyclic voltammograms upon raising the sweep rate (Figure 2b). Using previously described theoretical results, one obtains as an approximate value:

$$D_E(C_p^\circ)^2 \approx 10^{-15} \text{ M}^2 \text{ cm}^{-4} \text{ s}^{-1}$$

A more precise evaluation can be obtained using potential step chronoamperometry with sufficient excursion of the potential (from 0.2 to 1.2 V in oxidation and from 1.2 to 0.2 V in reduction). Examples of the resulting Cottrell plots are shown in Figure 3. From the average values of their slopes one obtains:^{2b}

$$D_E(C_p^\circ)^2 = 2.9 \times 10^{-15} \text{ M}^2 \text{ cm}^{-4} \text{ s}^{-1}$$

(20) The activity coefficients of the oxidized and reduced forms are expressed as:^{9b}

$$\gamma_P = \exp[-(a_{PP}C_P + a_{PQ}C_Q)]$$

$$\gamma_Q = \exp[-(a_{QQ}C_Q + a_{QP}C_P)]$$

the interaction of the two ions with the nonelectroactive ions being incorporated in the standard potential E_{PQ}° .

(18) Lavron, E. *Electroanalytical Chemistry*; Bard, A. J., Ed.; Marcel Dekker, New York, 1983; Vol. 12, pp 53-157.

(19) Andrieux, C. P.; Savéant, J. M. *J. Electroanal. Chem.* **1980**, *111*, 377.

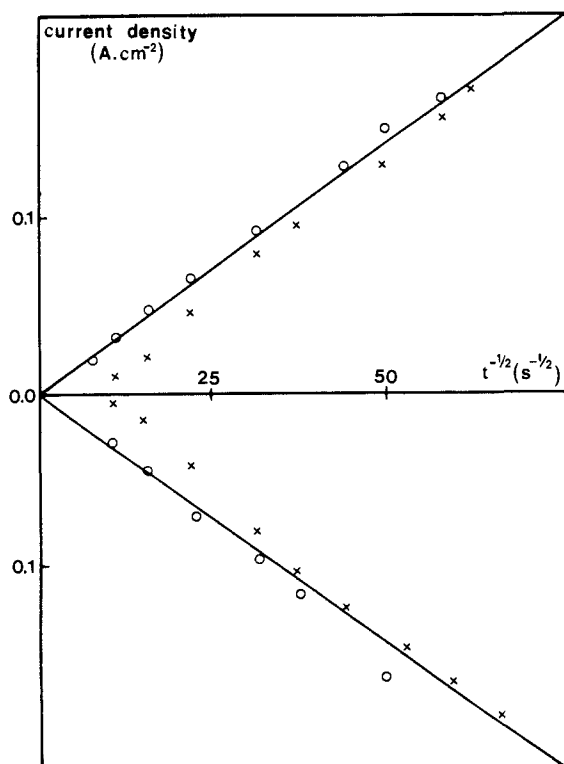


Figure 3. Potential step chronoamperometry of the ruthenium film in 0.1 M HCl. Potential excursion from 1.2 to 0.2 V on the cathodic side; from 0.2 to 1.2 V on the anodic side. Γ_p° (M cm^{-2}): 1.05×10^{-8} (O), 3.2×10^{-9} (X).

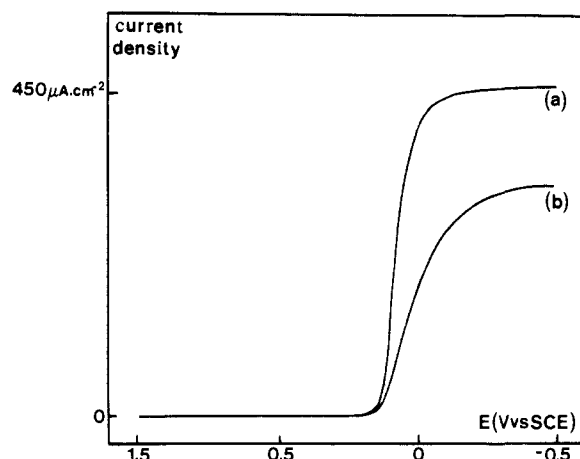


Figure 4. RDEV of the reduction of Fe(III) (1 mM) in 0.1 M HCl: (a) at a carbon electrode covered with a polyhydroxyphenazine film ($\Gamma = 6 \times 10^{-9} \text{ M cm}^{-2}$); (b) at the same electrode with additional coating of a ruthenium polymer film ($\Gamma_p^\circ = 10^{-8} \text{ M cm}^{-2}$). Rotation rate: 1000 rpm.

which leads to the expression of $i_{E,8}$ the current density characterizing the charge propagation, given in Table I, which we will use in the analysis of the catalytic processes by RDEV as described in the next sections.²¹

Diffusion of Iron(III) across the Polymer Coating. Another important parameter of the analysis of the catalytic processes is the diffusion rate of the substrate across the coating, as expressed, for example, by the corresponding characteristic current density.⁸

(21) (a) If we assumed that the film thickness in solution is not very different from what it is in the dry state,^{21b} $C_p^\circ \approx 10 \text{ mol L}^{-1}$ and thus $D_E = 2.9 \times 10^{-9} \text{ cm}^2 \text{ s}^{-1}$. (b) More systematic studies of charge propagation in similar polymers, carried out in concentrated HClO_4 , showed, using interferometry thickness measurements,^{21c} that this assumption leads to a correct order of magnitude for D_E . (c) Andrieux, C. P.; Gampp, H.; Savéant, J. M.; Vos, J. G., paper in preparation.

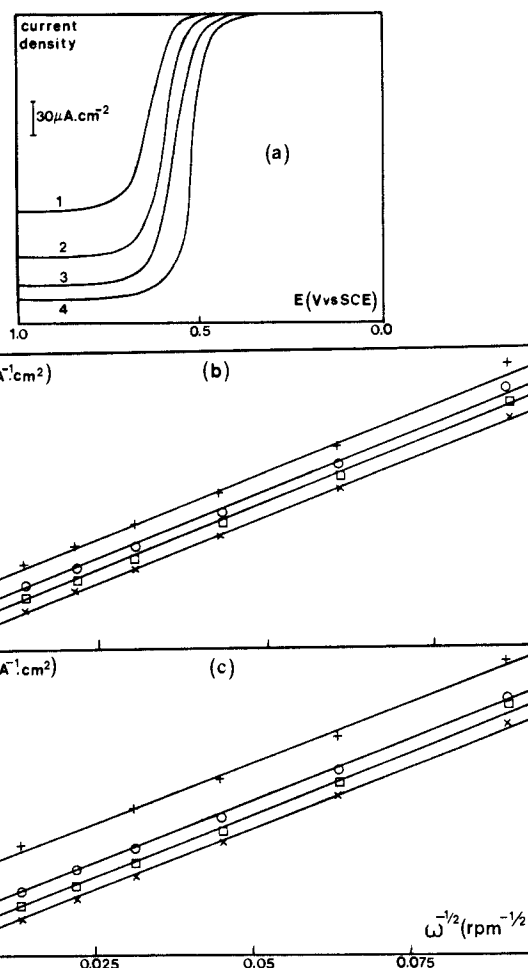


Figure 5. Oxidation of Fe(II) in 0.1 M HCl mediated by the ruthenium polymer. RDEV data. (a) Current density-potential curves at $\omega = 250$ rpm for Γ_p° (M cm^{-2}): 8×10^{-11} (1), 3.1×10^{-10} (2), 1.6×10^{-9} (3), 8.6×10^{-9} , and 2.4×10^{-8} (4) (Fe(II) concn: 1 mM). (b and c): Koutecky-Levich plots of the plateau current density for Γ_p° (M cm^{-2}): 1.4×10^{-10} (+), 2.5×10^{-10} (O), 6.7×10^{-10} (□), 2.9×10^{-9} (X) for two Fe(II) concentrations, 0.1 mM (b) and 1 mM (c).

Table I. Characteristics of the Mediation of the Fe(III)/Fe(II) Oxido-Reduction by the Ruthenium Polymer Coating in 0.1 M HCl

Characteristic Current Densities ^{a,8} (A cm^{-2}) ^b	
i_A	$1.42 \times 10^{-2} C_A^\circ \omega^{1/2}$
i_E	$2.9 \times 10^{-10} / \Gamma_p^\circ$
i_S	$1.35 \times 10^{-8} C_A^\circ / \Gamma_p^\circ$
i_{k_+}	$4.5 \times 10^9 C_A^\circ \Gamma_p^\circ$
i_{k_-}	$1.1 \times 10^6 C_A^\circ \Gamma_p^\circ$
Characteristics of the Catalytic Reaction 1	
equilibrium constant:	$K = 6 \times 10^3$
rate constant:	$k k_+ = 4.5 \times 10^4 \text{ M}^{-1} \text{ L s}^{-1}$

$$^a i_E = FD_E C_p^\circ / \phi = FD_E C_p^{02} / \Gamma_p^\circ, \quad i_S = FD_S \kappa C_A^\circ / \phi = F \kappa D_S C_A^\circ C_p^\circ / \Gamma_p^\circ, \quad ^b C_A^\circ \text{ in M L}^{-1}, \Gamma_p^\circ \text{ in M cm}^{-2}, \omega \text{ in rpm.}$$

This was determined from the following experiments.

As discussed in more detail in the next section, the catalytic current for the mediation of the Fe(III) \rightarrow Fe(II) reaction by the Ru(III)/Ru(II) couple is small. For example, with a millimolar concentration of Fe(III) and a $\Gamma_p^\circ = 10^{-8} \text{ M cm}^{-2}$ coating, the catalytic current is negligible vis-à-vis the current corresponding to the direct reduction of Fe(III) (the ratio is predicted to be 2% on the basis of the analysis developed in the next section). Under these conditions, the direct reduction current of Fe(III) at such a polymer coated electrode could, in principle, be a measure of the diffusion rate of Fe(III) through the coating. Unfortunately, the reduction of Fe(III) at a bare carbon electrode in 1 M HCl

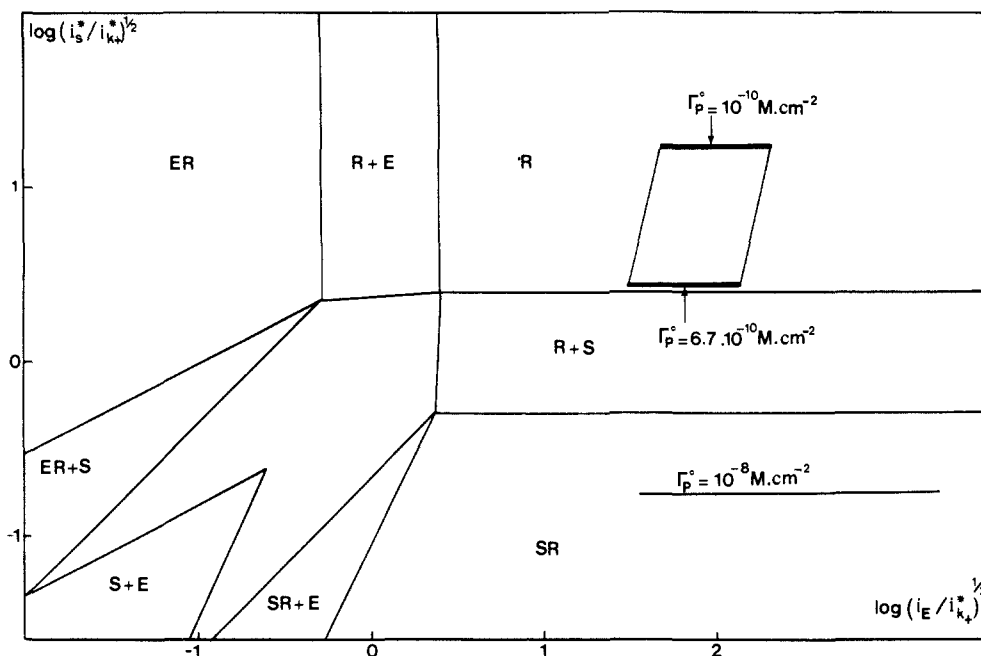


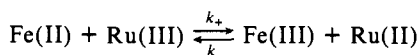
Figure 6. Kinetic zone diagram showing the kinetic control of the process taking place in the coating as a function of the film thickness (through Γ_p^0). The extreme points of the segments in the R region are for $\omega = 1000$ rpm and $C_A^0 = 0.1$ mM (right-hand side) and $C_A^0 = 2$ mM (left-hand side).

does not give rise to a well-defined wave, thus preventing a meaningful determination of this diffusion rate. To overcome this difficulty we deposited on the electrode surface a first film of polymeric 1-hydroxyphenazine which has the property of catalyzing the reduction of Fe(III).²² A second film of the ruthenium polymer was then deposited on top of the phenazine film and the resulting RDEV wave recorded. The results are shown in Figure 4. The magnitude of the substrate diffusion characteristic current density, i_s ,⁸ is then obtained from the decrease of the plateau current induced by the coating of the ruthenium polymer film according to:

$$\frac{1}{i_L} = \frac{1}{i_A} + \frac{1}{i_S}$$

(where i_L is the observed plateau current density and i_A the current density observed in the absence of the ruthenium polymer which corresponds to the solution diffusion-controlled reduction of iron(III)). The resulting expression of i_S is given in Table I.²³

Mediation of the Fe(II) - e⁻ ⇌ Fe(III) Reaction by the Ruthenium Polymer Coatings. The electrochemical oxidation of Fe(II) into Fe(III) in 1 M HCl at a bare carbon electrode (in millimolar concentrations, under N₂) does not give rise to any defined wave in the potential region of the polymer Ru(III)/Ru(II) couple although this ($E_{PQ}^0 = 0.680$ V vs. SCE) is significantly more positive than the Fe(III)/Fe(II) standard potential in this medium. The latter quantity, E_{AB}^0 , is equal to 0.460 V vs. SCE.²⁴ The oxidation of Fe(II) by Ru(III)



is thus a down-hill reaction with a driving force of 220 mV.

As seen in Figure 5a, a wave corresponding to the mediated oxidation of iron(II) according to the above equation does appear

in the potential region where Ru(II) is oxidized to Ru(III) in the polymer coating.

With thick coatings ($\Gamma_p^0 > 3 \times 10^{-9}$ M cm⁻²) the plateau current becomes independent of Γ_p^0 and corresponds to total catalysis in the sense that it is entirely controlled by the diffusion of Fe(II) from the bulk of the solution to the solution/coating boundary ($i_L = i_A$ according to the notations defined in footnote 8). Kinetic limitations from phenomena taking place within the film appear for thinner coatings: the plateau current density decreases below i_A and the half-wave potential shifts positively.

Since the equilibrium constant of eq 1, $K = 6 \times 10^3$, is largely in favor of the right-hand side, we can analyze the variations of the plateau current density, i_L , with the rotation rate ω , the Fe(II) concentration in the bulk of the solution, C_A^0 , and the amount of ruthenium per unit surface area, Γ_p^0 , in terms of the theory previously developed for an irreversible catalytic reaction.^{4d-f,5a}

In this purpose, the RDEV plateau current data are displayed in the form of i_L^{-1} vs. $\omega^{-1/2}$ plots (Figure 5b, c). Linear plots are obtained, the slopes of which are inversely proportional to C_A^0 and the intercept inversely proportional to Γ_p^0 at low ruthenium polymer coverages. This indicates that the kinetic control within the film corresponds to an "R" situation,^{4d-f} i.e., to the catalytic reaction 1 being the sole rate-determining step while the charge propagation and the diffusion of the substrate are fast enough not to interfere kinetically.

That this conclusion is compatible with the estimations made in the previous sections of the characteristic current densities featuring the two latter phenomena (Table I) is shown in Figure 6. As described previously,^{4f,h} a kinetic zone diagram can be constructed defining the zones for the various types of kinetic control of the catalytic process in terms of the two parameters $i_S^*/i_{k_+}^*$ and $i_E/i_{k_+}^*$, where i_S^* and $i_{k_+}^*$ are defined from i_S and i_{k_+} as:

$$i_S^* = i_S \left(1 - \frac{i_L}{i_A} \right), \quad i_{k_+}^* = i_{k_+} \left(1 - \frac{i_L}{i_A} \right)$$

It is clearly seen that, for ruthenium coverages in the range $10^{-10} - 6.7 \times 10^{-10}$ M cm⁻² corresponding to i_L values that are appreciably below i_A , the kinetic control is of the "R" type.

For larger values of the film thickness (as represented by Γ_p^0),

(22) Haas, O.; Zumbrunnen, H. R. *Helv. Chim. Acta* **1981**, *64*, 854.

(23) (a) We take that same value of i_S for both Fe(III) and Fe(II) assuming that their diffusion coefficients and partition coefficients in the coating are not very different. This approximation is not as crude as it may look at first sight. As results from the discussion below, the polymer offers a rather open structure allowing the penetration of a large amount of solvent and supporting electrolyte. Under these conditions, the environment experienced by the Fe(III) and Fe(II) ions is not very much different from what it is in the solution. (b) This corresponds to a value of the diffusion coefficient of Fe(III) through the film, D_S ,⁷ of the order of 1.3×10^{-10} cm² s⁻¹.²¹

(24) Ateya, B. G.; Austin, L. G. *J. Electrochem. Soc.* **1973**, *120*, 1217.

the plateau current density tends toward i_A . At the same time, the kinetic control tends to shift from the "R" type to the "SR" type (Figure 6) because i_S and i_{k_+} are decreasing and increasing functions of Γ_P° , respectively.⁷ For, e.g., $\Gamma_P^\circ = 10^{-8}$ M cm⁻², the kinetic control is entirely of the "SR" type; i.e., the catalytic reaction takes place in a reaction layer adjacent to the coating/solution boundary, the thickness of which (μ) is small vis-à-vis that of the coating (ϕ):^{4d}

$$\frac{\mu}{\phi} = (i_S/i_{k_+})^{1/2} = 0.17$$

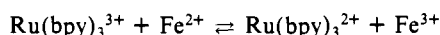
Under these conditions, the plateau current density is given by:^{4d-f}

$$\frac{1}{i_L} = \frac{1}{i_A} + \frac{1}{(i_{k_+}i_S)^{1/2}}$$

The second term is always much smaller than the first (for example, at 1000 rpm $i_A/(i_{k_+}i_S)^{1/2} = 6 \times 10^{-2}$ as derived from the data of Table I) which matches the observation that catalysis is then practically total.

Thus, the catalytic process, far from being a surface reaction, encompasses a substantial portion of the coating: from the entire coating to 20% of it when passing from the smallest to the largest ruthenium polymer coverages.

The value of the rate constant of the catalytic reaction 1 can be obtained from the value of the corresponding catalytic current density, i_{k_+} ⁸ (Table I). A value of 4.5×10^4 M⁻¹ L s⁻¹ for k_+ is then found which is worth comparing with the values already determined for a similar reaction in solution:



In pH 3 HClO₄ solutions, the rate constant was found to be 8.5×10^5 M⁻¹ L s⁻¹ and 3.4×10^6 M⁻¹ L s⁻¹ in the absence and presence of poly(vinyl sulfate) respectively.²⁵ The equilibrium constant is then 6×10^8 corresponding to a driving force of 510 mV instead of 220 mV in the present case. Taking this difference in driving force into account, according to a Marcus relationship with a 0.5 transfer coefficient, results in values in the range 3×10^3 – 10^4 M⁻¹ L s⁻¹. Although this represents a rather crude approximation, we can thus conclude that the rate constant of the reaction within the polymer coating is of the same order of magnitude as it appears to be in solution.

Let us now discuss the catalytic process in terms of the potential location of the catalytic wave and its variations with the experimental parameters. Upon increasing the ruthenium coverage, the catalytic wave first shifts negatively while its height increases and then stops to shift when its height has reached its maximal value (Figure 5a). From what has been discussed above, these variations in height features, in the framework of a "R + S" kinetic control, the passage from a "R" to a "SR" situation. Whether the concomitant variations of the half-wave potential fit with this evolution in the kinetic control is the question we address now. A simple extension of the previously derived theory regarding the half-wave potentials^{5a} leads to the following equation which expresses $E_{1/2} - E_{PQ}^\circ$ as a function of two parameters: i_{k_+}/i_A and $i_A/(i_{k_+}i_S)^{1/2}$ (the derivation is given in the Appendix):

$$\frac{1}{1 + \exp\left[\frac{F}{RT}(E_{1/2} - E_{PQ}^\circ)\right]} \times \frac{1}{\tanh\left[\frac{i_A}{(i_{k_+}i_S)^{1/2}} \frac{i_{k_+}}{i_A} \left\{1 + \exp\left[-\frac{F}{RT}(E_{1/2} - E_{PQ}^\circ)\right]\right\}^{1/2}\right]} = \frac{1}{i_A} + \frac{2}{\tanh\left[\frac{i_A}{(i_{k_+}i_S)^{1/2}} \frac{i_{k_+}}{i_A}\right]} \quad (2)$$

When $i_{k_+}/i_A \rightarrow 0$, the "R" situation is reached, corresponding to:

$$E_{1/2} = E_{PQ}^\circ - \frac{RT}{F} \ln\left(1 + \frac{i_{k_+}}{i_A}\right)$$

Since i_{k_+} is proportional to Γ_P° and i_A is independent of Γ_P° , the half-wave potential is predicted to shift negatively as the ruthenium coverage increases. Upon increasing the film thickness, the catalytic efficiency is thus predicted to increase in two ways: the catalytic current increases and the reaction takes place at a less and less positive potential, i.e., comes closer and closer to the standard potential of the substrate redox couple.

Conversely, when $i_{k_+}/i_A \rightarrow \infty$, the "SR" situation is reached. Then:

$$E_{1/2} = E_{PQ}^\circ - \frac{RT}{F} \ln\left[\frac{i_{k_+}i_S}{i_A^2} + 4\frac{(i_{k_+}i_S)^{1/2}}{i_A} + 3\right]$$

$(i_{k_+}i_S)^{1/2}/i_A$ is independent of the catalyst coverage. This shows that upon increasing Γ_P° the half-wave potential stops to vary with Γ_P° . It is thus useless to continue increasing the catalyst coverage since the current stops to increase and the potential stops to shift negatively.

These trends match qualitatively what is seen in Figure 5a. The whole theoretical variations of the half-wave potential are summarized in Figure 7. Comparison of the experimental values with the theoretical working curves shows a good quantitative agreement.

One conclusion that can be derived from the above analysis concerns the optimization of the film thickness. It is seen that over a coverage of 10^{-8} M cm⁻² there is very little to gain by a further increase of the coverage from the point of view of both the current height and the potential at which the catalytic reaction can be carried out. It is remarkable that "total catalysis" is then reached in the sense that the current is solely limited by the transport of the substrate from the bulk of the solution to the solution/coating boundary.

Mediation of the Fe(III) + e⁻ ⇌ Fe(II) Reaction by the Ruthenium Polymer Coatings. Catalysis of the reduction of Fe(III) by the ruthenium polymer coating occurs in the potential region of the Ru(III)/Ru(II) couple as seen in Figure 8a. As expected from the fact that the catalytic reaction (backward eq 1) is an uphill process (by 220 mV), the catalytic currents are small. Relatively large concentrations of Fe(III) (5 mM) had to be used to make the detection of the catalytic wave possible.

Since the catalytic step is anticipated to be slow (k_- is of the order of 1–10 M⁻¹ L s⁻¹, as results from the values of κk_+ and K determined in the preceding section), it is expected that the kinetic control be of the "R" type. This is indeed what is found experimentally as can be seen from the Koutecky–Levich plots shown in Figure 8b. The intercept is approximately proportional to the inverse of Γ_P° as expected for an "R"-type kinetic control:

$$\frac{1}{i_L} = \frac{1}{i_A} + \frac{1}{i_{k_-}}$$

with

$$i_{k_-} = Fk_- \kappa C_A^\circ \Gamma_P^\circ$$

From the values of the intercept, the numerical expression of i_{k_-} given in Table I is found.

From the ratio of i_{k_+} and i_{k_-} (Table I), we find a value of the equilibrium constant of eq 1, $K = 4 \times 10^3$ which is consistent with the value derived from the difference between the standard potentials of the Ru(III)/Ru(II) and Fe(III)/Fe(II) couples, $K = 6 \times 10^3$.

It seems surprising at first sight that the Ru(III)/Ru(II) couple

(25) Meisel, D.; Rabani, J.; Meyerstein, D.; Matheson, M. S. *J. Phys. Chem.* 1978, 82, 985.

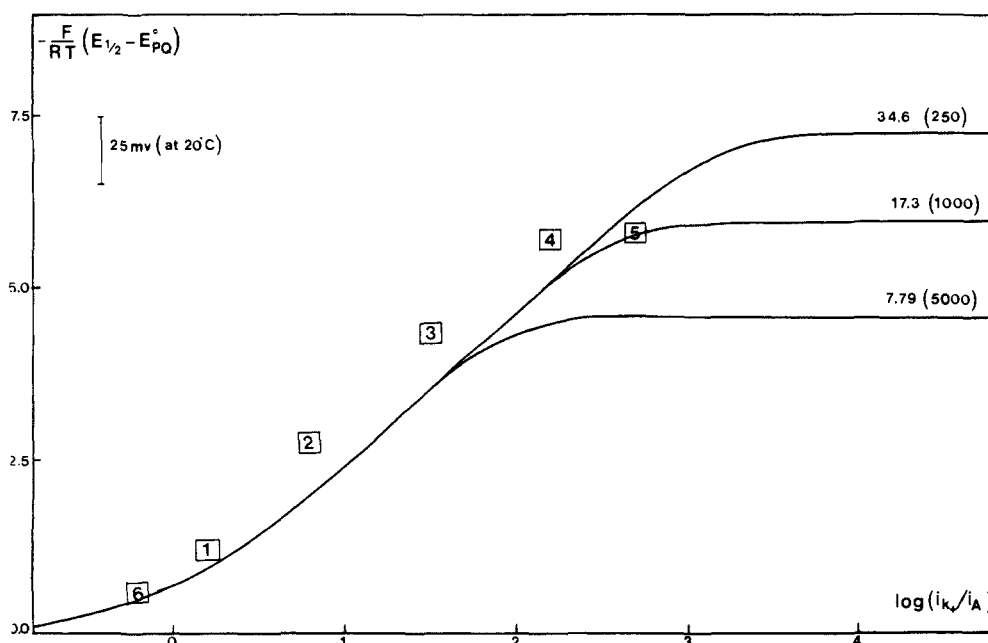


Figure 7. Variations of the half-wave potential under the "R + S" kinetic control with the two parameters i_{k+}/i_A and $(i_{k+}i_S)^{1/2}/i_A$. Theoretical variations: (full lines) the number on each curve is the value of $(i_{k+}i_S)^{1/2}/i_A$; the number between parentheses is the corresponding value of ω in rpm (from the data listed in Table I): $(i_{k+}i_S)^{1/2}/i_A = 8.6 \omega^{-1/2}$. The numbered open squares are the experimental data: from 1 to 5, $\omega = 250$ rpm and $\Gamma_P^0 = 8 \times 10^{-11}$, 3.1×10^{-10} , 1.6×10^{-9} , 8.6×10^{-9} , 2.4×10^{-8} M cm⁻²; for 6, $\omega = 5000$ rpm, $\Gamma_P^0 = 1.4 \times 10^{-10}$ M cm⁻².

is able to catalyze the reduction of Fe(III) since the first couple has a standard potential positive (by 220 mV) to the second couple. That thermodynamics is not in fact violated can be seen in Figure 8a: the catalytic waves have an half-wave potential which is shifted negatively toward the Fe(III)/Fe(II) standard potential to such an extent that the catalytic current is, at any potential, smaller than the current that would correspond to an infinitely fast reduction of the same amount of Fe(III) at a bare electrode (dotted line in Figure 8b).²⁶

The negative shift of the half-wave potential of the catalytic wave upon increasing the ruthenium polymer coverage is also in accord with what is predicted from the theory:^{5a}

$$E_{1/2} = E_{PQ}^0 + \frac{RT}{F} \ln \left(\frac{1 + \frac{i_{k-}}{i_A}}{1 + \frac{i_{k+}}{i_A}} \right)$$

The following results are found:

Γ_P^0 (M cm ⁻²)	$E_{1/2}^{\text{theor}}$	$E_{1/2}^{\text{exptl}}$ (V vs. SCE)
3.6×10^{-8}	0.53 ₃	0.53 ₅
8.2×10^{-9}	0.56 ₉	0.56 ₀

showing quite satisfactory agreement between the experimental data and the predicted values.

Conclusions

The [Ru(bpy)₂Cl-poly(4-vinylpyridine)] polymer investigated in this study is able to catalyze the oxidation of Fe(II) to Fe(III) in 1 M HCl quite efficiently. Total catalysis giving rise to plateau currents solely controlled by solution mass transport is reached for surface coverage of the order of 10⁻⁸ M cm⁻². Catalysis then occurs at a half-wave potential which is only 75 mV positive to the Fe(II)/Fe(III) standard potential. Up to this value of the surface coverage, which appears as an optimum both in terms of

current and potential catalytic efficiencies, quite substantial portions of the coating are catalytically active. In this respect, the investigated system is a good example of the interest of redox polymer coatings in the catalysis of electrochemical reactions deriving from the three-dimensional dispersion of the catalytic centers.

The polymer also catalyzes, although much less efficiently, the reduction of Fe(III) to Fe(II) in the same reaction medium in spite of the fact that the Ru(III)/Ru(II) standard potential is positive to that of the Fe(III)/Fe(II) couple.

In both cases, there is a quite satisfactory agreement between the experimental data and the theoretical predictions based on previously developed kinetic models. This further experimental demonstration of the validity of these kinetic models concerns the analysis of the variations of the catalytic current but also the variations of the potential location of the catalytic waves with the various experimental parameters.

Experimental Section

The procedure for preparing [Ru(bpy)₂Cl-poly(4-vinylpyridine)] has been described in detail elsewhere.^{17a} The glassy carbon electrodes were prepared using cylindrical rods ($\phi = 3$ mm) from Sigr AG BRD, which were introduced in a Kelef cylinder with a milled hole of $\phi = 2.95$ mm heated at 160 °C. These disk electrodes were then polished with a 1- μ m diamond paste. The electrodes were spin-coated from a methanolic solution of the polymer (10 mg of the polymer in 10 mL methanol). About 1- μ L was deposited on the GC disk which was spinned at 3000 rpm while being maintained in an upward position. Quite homogeneous films could be prepared by this technique. The coverage was checked by recording the cyclic voltammogram in 1 M HCl at low sweep rate. If the coverage was not sufficient, the electrode was rinsed with distilled water and the procedure repeated until the desired coverage was reached. The exact value of the surface coverage was obtained from integration of the low sweep rate cyclic voltammograms.

The reference electrode was a saturated calomel electrode and the temperature of the experiments was 20 °C.

Rotating disk voltammograms, cyclic voltammograms, and potential-step current-time curves were obtained using a PAR (175) or a Taccussel (GSTP) function generator and a home-built potentiostat equipped with positive feedback compensation.²⁷ The RDEV curves were recorded on a XY chart recorder (Ifelec 2502) at a potential scanning rate of 200 mV/mn. The same recorder was used in cyclic voltammetry up to a sweep rate of 0.5 V s⁻¹. Over this value a Nicolet (3091) storage oscilloscope was used as well as in all the potential-step experiments.

(26) A similar situation has been previously encountered with another ruthenium polymer in a case where, however, the substrate was not able to penetrate the film.^{9a}

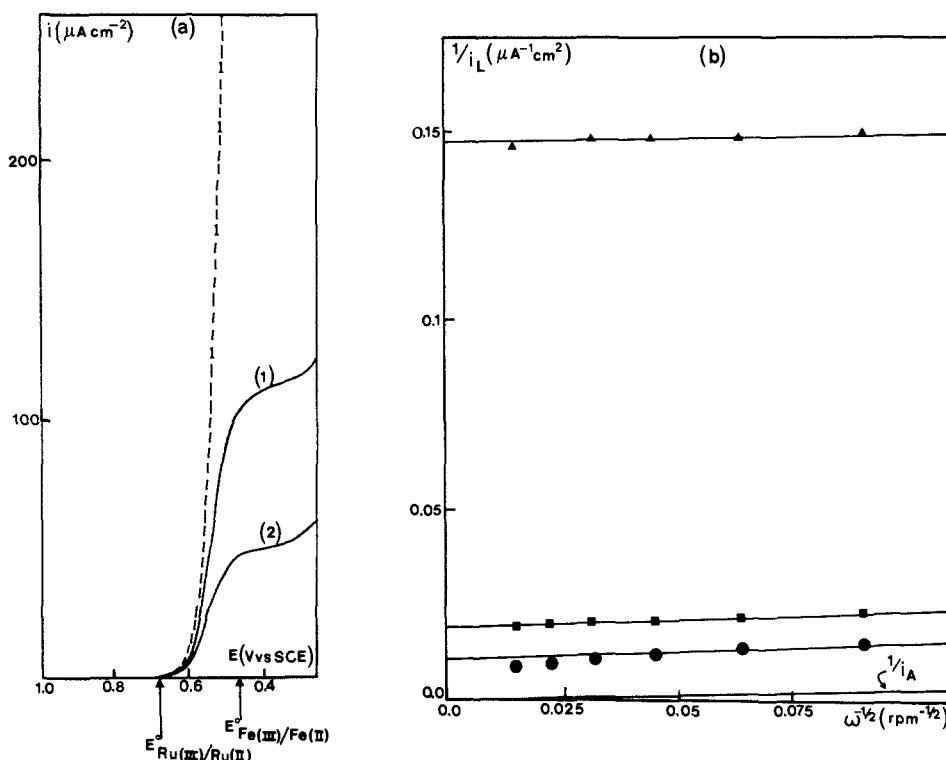


Figure 8. Mediation of the Fe(III) + e \rightleftharpoons Fe(II) reduction in 0.1 M HCl (Fe(III) concn 5 mM). (a) RDE voltammograms at 1000 rpm (solid lines) for $\Gamma_p^\circ = 3.6 \times 10^{-8}$ (1) and 8.2×10^{-9} (2) M cm^{-2} . Dotted line: theoretical voltammogram corresponding to an infinitely fast reduction of Fe(III) at a bare electrode. (b) Koutecký-Levich plots for Γ_p° : 3.6×10^{-8} (●), 8.2×10^{-9} (■), 8.1×10^{-10} (▲) M cm^{-2} . i_A represents the Levich current.

Acknowledgment. O.H. wishes to thank the C.I.E.S. for a fellowship making possible his stay in the Laboratoire d'Electrochimie Moléculaire de l'Université de Paris 7. We are indebted to J. G. Vos for supplying several samples of the investigated polymer.

Appendix

By use of the notations defined in footnote 8, the problem to be solved can be formulated as:^{4,5}

for $0 < x < \phi$

$$D_S \frac{d^2 C_A}{dx^2} - k C_A C_Q = 0$$

for $x = \phi$

$$(C_A)_{\phi^-} = \kappa (C_A)_{\phi^+}, D_S \left(\frac{dC_A}{dx} \right)_{\phi^-} = D \left(\frac{dC_A}{dx} \right)_{\phi^+}, \left(\frac{dC_A}{dx} \right)_{\phi^+} = \frac{C_A^\circ - (C_A)_\phi}{\delta}$$

for $x = 0$

$$\frac{dC_A}{dx} = 0, C_Q = \frac{C_P^\circ}{1 + \exp(-\xi)}$$

The current density being given by:

$$\frac{|i|}{F} = -D_E \left(\frac{dC_Q}{dx} \right)_0 = D_S \left(\frac{dC_A}{dx} \right)_{\phi^-} = D \left(\frac{dC_A}{dx} \right)_{\phi^+}$$

(x is the distance from the electrode; C_A and C_Q are the space-dependent concentrations of A and Q; $\xi = \pm(F/RT)(E - E_{PQ}^\circ)$, + for oxidation, - for reduction, is a dimensionless measure of the electrode potential, taking E_{PQ}° as a reference).

Since "R + S" conditions are dealt with, C_Q is a constant throughout the film, equal to its value at the electrode surface.^{4d,5a}

It follows that:

$$\frac{d^2 a^*}{dy^2} - \frac{i_k^*}{i_S^*} \frac{a^*}{1 + \exp(-\xi)} = 0$$

with as boundary conditions $(da^*/dy)_0 = 0$, $a_1^* = 1$, and as definition of the new dimensionless variables:

$$y = \frac{x}{\phi}, a^* = \frac{a}{|i|}, i_k^* = i_k \left(1 - \frac{|i|}{i_A} \right), i_S^* = i_S \left(1 - \frac{|i|}{i_A} \right)$$

Integration leads to:

$$\frac{|i|}{i_S^*} = \left[\frac{i_k^*}{i_S^*} \frac{1}{1 + \exp(-\xi)} \right]^{1/2} \tanh \left[\frac{i_k^*}{i_S^*} \frac{1}{1 + \exp(-\xi)} \right]^{1/2}$$

i.e.,

$$\frac{1}{|i|} = \frac{1}{i_A} + \frac{1}{\frac{(i_{k+} i_S)^{1/2}}{[1 + \exp(-\xi)]^{1/2}} \tanh \left[\frac{i_{k+}}{i_S} \frac{1}{1 + \exp(-\xi)} \right]^{1/2}}$$

the plateau current density being given by:

$$\frac{1}{|i_L|} = \frac{1}{i_A} + \frac{1}{(i_{k+} i_S)^{1/2} \tanh \left(\frac{i_{k+}}{i_S} \right)^{1/2}}$$

The half-wave potential is then obtained by equating $|i|$ to $|i_L|/2$ using the two above equations leading to eq 2 in the text.

Registry No. Fe, 7439-89-6; HCl, 7647-01-0; carbon, 7440-44-0; polyhydroxyphenazine, 105103-78-4.